Meteorology and Atmospheric Physics
https://doi.org/10.1007/s00703-018-0588-3

ORIGINAL PAPER

An improvement of the retrieval of temperature and relative humidity profiles from a combination of active and passive remote sensing

Yunfei Che[1] · Shuqing Ma[2] · Fenghua Xing[3] · Siteng Li[4] · Yaru Dai[5]

Received: 14 September 2017 / Accepted: 17 February 2018

Abstract
This paper focuses on an improvement of the retrieval of atmospheric temperature and relative humidity profiles through combining active and passive remote sensing. Ground-based microwave radiometer and millimeter-wavelength cloud radar were used to acquire the observations. Cloud base height and cloud thickness determinations from cloud radar were added into the atmospheric profile retrieval process, and a back-propagation neural network method was used as the retrieval tool. Because a substantial amount of data are required to train a neural network, and as microwave radiometer data are insufficient for this purpose, 8 years of radiosonde data from Beijing were used as the database. The monochromatic radiative transfer model was used to calculate the brightness temperatures in the same channels as the microwave radiometer. Parts of the cloud base heights and cloud thicknesses in the training data set were also estimated using the radiosonde data. The accuracy of the results was analyzed through a comparison with L-band sounding radar data and quantified using the mean bias, root-mean-square error (RMSE), and correlation coefficient. The statistical results showed that an inversion with cloud information was the optimal method. Compared with the inversion profiles without cloud information, the RMSE values after adding cloud information reduced to varying degrees for the vast majority of height layers. These reductions were particularly clear in layers with clouds. The maximum reduction in the RMSE for the temperature profile was 2.2 K, while that for the humidity profile was 16%.

1 Introduction

The acquisition of radiosonde observations is fundamental for generating atmospheric profiles, but such observations are limited by their cost, sparse temporal sampling, and logistical difficulties. Over the past 20 years, many researchers have shown that ground-based remote sensing is capable of measuring atmospheric profiles in the lower troposphere (Solheim et al. 1998; Ware et al. 2003). Therein, the ground-based microwave radiometer (MWR) is an important instrument for retrieving humidity and temperature profiles. It can provide continuous observations, thereby providing data on the complete process of an entire weather event as it evolves (Candlish et al. 2012; Sanchez et al. 2013; Ware et al. 2013).

Through a number of studies, it has been shown that the performance of the MWR in retrieving atmospheric profiles is good under clear conditions. However, the retrievals of such profiles, especially relative humidity profiles, tend to be far worse under cloudy or rainy conditions, with some extreme cases yielding acutely obvious errors (Chan 2009). Thus, various researchers have attempted to obtain higher accuracy atmospheric parameters from combined vertical observations. For instance, Stankov (1996), Bianco et al. (2005) and Klaus et al. (2006) combined radar wind profiler and MWR measurements to estimate atmospheric humidity profiles. Brandau et al. (2010), Frisch et al. (1995) and Lohnert et al. (2001) evaluated the liquid water content of clouds through a combination of millimeter-wavelength radar and MWR data, and demonstrated that significant improvements

Responsible Editor: S.-W. Kim.

✉ Yunfei Che
cheyf@cam.gov.cn

[1] Key Laboratory for Cloud Physics, Chinese Academy of Meteorological Sciences, Beijing 100081, China

[2] Meteorological Observation Center of China Meteorological Administration, Beijing 100081, China

[3] Hainan Institute of Meteorological Sciences, Haikou 570203, Hainan, China

[4] Beijing Municipal Meteorological Observation Center, Beijing 100089, China

[5] National Space Science Center, Chinese Academy of Sciences, Beijing 100029, China

Published online: 10 March 2018

could be made in the retrieval of cloud liquid water profiles by adopting such an approach. Lijegren and Clothiaux (2001) used MWR and cloud temperature observations to retrieve for cloud liquid water profiles. Han and Westwater (1995) developed a technique to derive atmospheric profiles from an integrated system composed of a microwave radiometer, a variety of surface meteorological instruments, a laser ceilometer, and a radio acoustic sounding system (RASS).

Most previous studies were conducted to improve the retrieval of the cloud liquid water content from combined MWR and cloud radar measurements. In terms of the improvement of humidity profiles, more studies used a combination of MWR and wind profiler radar data. However, cloud parameters can also impact the MWR retrieval of atmospheric temperature and humidity profiles, as the presence of clouds can lead to obvious changes in the brightness temperature (BT) measured by the MWR relative to clear-sky conditions. Meanwhile, the relative humidity can increase rapidly within the cloud layer, and the temperatures therein may also change. Thus, accurate cloud information is necessary for MWR retrieval algorithms. Frate and Schiavon (1998) proved that neural networks are flexible and demonstrate good capabilities for exploiting information provided by other instruments. Solheim et al. (1998) distinguished data according to different cloud conditions when they used a neural network; for clear condition, the input nodes include brightness temperatures, surface temperature, vapor density, and pressure; for cloudy conditions, the cloud base information was represented by ones in a set of 47 height bins at the same heights as the output profile.

The present study combines active and passive remote sensing-based techniques previously presented in the literature with the aim of improving retrieval algorithms using ground-based MWR observations under cloudy conditions. Atmospheric profiles were detected through a combination of ground-based MWR and millimeter-wavelength cloud radar (MWCR) observations. The retrieval tool used was a back-propagation neural network (BPNN). The cloud information acquired using the cloud radar was added during the MWR atmospheric profile retrieval process, and the accuracy of the MWR retrieval was analyzed through a comparison with L-band sounding radar data. The impact of including cloud information during the retrieval of atmospheric profiles was then assessed.

2 Data sources and pre-treatment

2.1 Data sources

The data used in this study include radiosonde data, BT, the retrieval product of the MWR, in addition to MWCR cloud base height and thickness data. The experimental site is the Beijing Nanjiao Meteorological Observatory. The radiosonde data with a temporal resolution of 1 s were obtained from an L-band GTS1 digital radiosonde (Bian et al. 2011), the sounding balloon for which requires approximately 40 min to travel from 0 to 10 km above ground level. The MWR used in this study was the RPG-HATPRO model (Radiometer Physics GmbH). The RPG-HATPRO 14-channel ground-based MWR includes seven K-band frequency channels between 22 and 30 GHz and seven V-band channels between 51 and 59 GHz. The absolute BT accuracy is 0.5 K.

The MWCR was produced by the Meteorological Observation Center of the China Meteorological Administration and Xi'an Huateng Microwave Co. Ltd. The cloud radar is a vertically oriented solid-state Doppler radar with a working frequency of 35 GHz, a peak power of 4 W, and a sounding range of 12 km. It has a spatial resolution of 30 m and an adjustable temporal resolution between 1 and 60 s. The threshold of the MWCR reflectivity is – 30 dBz.

Ideally, to eliminate system errors as much as possible, the three instruments should collect their observations at the same time and location. However, the positions of the detectors among the instruments differed slightly because of limitations imposed by the experimental conditions. The distance between the MWR and the cloud radar was 61.75 m, the distance between the cloud radar and radiosonde was 162.37 m, and the distance between the MWR and radiosonde was 182.51 m. The training data set in this study was based on 8 years (from 2006 to 2013) of annual radiosonde data. Soundings were made twice daily (11:15 and 23:15 UTC).

The data collected during rainy or uncertain weather conditions were removed, because radiometer measurements become less accurate in the presence of a water film on the radome of the equipment in precipitating conditions (Chan 2009). A total of 2715 training samples were acquired; of those, 1626 were taken during clear-sky conditions and 1089 were taken during cloudy conditions. The test data set included 100 randomly selected groups of data during 2006–2013 that were not used for training in addition to 382 groups of sounding data from 2014 to January 2015 (excluding rainy conditions). It should be noted that the cloud base height and cloud thickness data between 2013 and 2015 were provided by the MWCR and the cloud information for the other samples was obtained by analyzing the relative humidity measurement from the radiosonde because of the insufficient amount of cloud radar data.

2.2 Pre-treatment of the sounding data

The training process required a substantial amount of cloud information, but not all of the samples could be matched to the information from the cloud radar, which had been running since 2013 only. Therefore, radiosonde data were used

to estimate the cloud parameters in some cases. This section describes the method used to determine the weather conditions from the radiosonde sounding data. In theory, clouds should form when the relative humidity reaches 100%; however, because of various factors such as the presence of condensation nuclei, clouds can form when the relative humidity reaches only approximately 85%. This study used 84% as the threshold for the relative humidity following the work of Wang et al. (1995). The specific methods used to determine the weather conditions were as follows.

If the relative humidity was consistently less than 84% from the ground to any height, the weather was classified as having clear-sky conditions. If the relative humidity was consistently greater than 84% from the ground to a height of 600 m, the weather was classified as rain. If the relative humidity was less than 84% near the ground, but stratification was observed with a relative humidity greater than 84%, the weather was classified as cloudy. Under cloudy conditions, the cloud base height and cloud-top height were determined based on the work of Wang and Rossow (1995).

The above method was used to filter the radiosonde data according to clear-sky and cloudy conditions and to obtain the cloud base height and thickness at the times of radiosonde observations under cloudy conditions.

2.3 Comparison of cloud parameters determined by the radiosonde and cloud radar

We used the cloud base height and cloud thickness estimated using the radiosonde data to supply the cloud information when cloud radar data were absent. However, to reduce the impacts of errors from the estimated cloud information on the accuracy of the retrieval, we verified the feasibility of the method by comparing 60 groups of cloud information estimated using the radiosonde data with simultaneous MWCR measurements. The results of the comparison are shown in Fig. 1.

In the sample statistics from the 60 groups of cloud information, there were five groups in which the clouds were shown to be present according to one instrument but not according to the other one. Because of the presence of condensation nuclei and ice crystals, the humidity might not have reached 84%, which could have caused the inability of the radiosonde to detect clouds. In addition, the cloud radar might have sometimes missed thin clouds within small cloud droplets.

Excluding these five groups of abnormal samples, the remaining 55 groups were used as statistical samples. The results of the comparison are as follows. For the cloud base height, the mean bias was 0.476 km and the correlation coefficient was 0.936. For the cloud thickness, the mean bias was 0.450 km and the correlation coefficient was 0.723.

To analyze the influence of cloud information error on the retrieval, we did a test experiment for the sensitivity about the uncertainty of cloud. In the test, we kept other parameter fixed, only modify the cloud height or cloud thickness, compared the difference between the output atmospheric profiles, and two cases are shown as follow.

In the case of Fig. 2, the cloud base height measured by cloud radar is 2523 m and thickness is 663 m. In (a) and (c), we keep other input parameters fixed, only modify the cloud base height to 3000, 3500, and 4000 m, and compare the change of the temperature and relative humidity profiles. In (b) and (d), the thickness is modified to 1000, 1500, and 2000 m. It should be noted that the cloud layer is artificially modified.

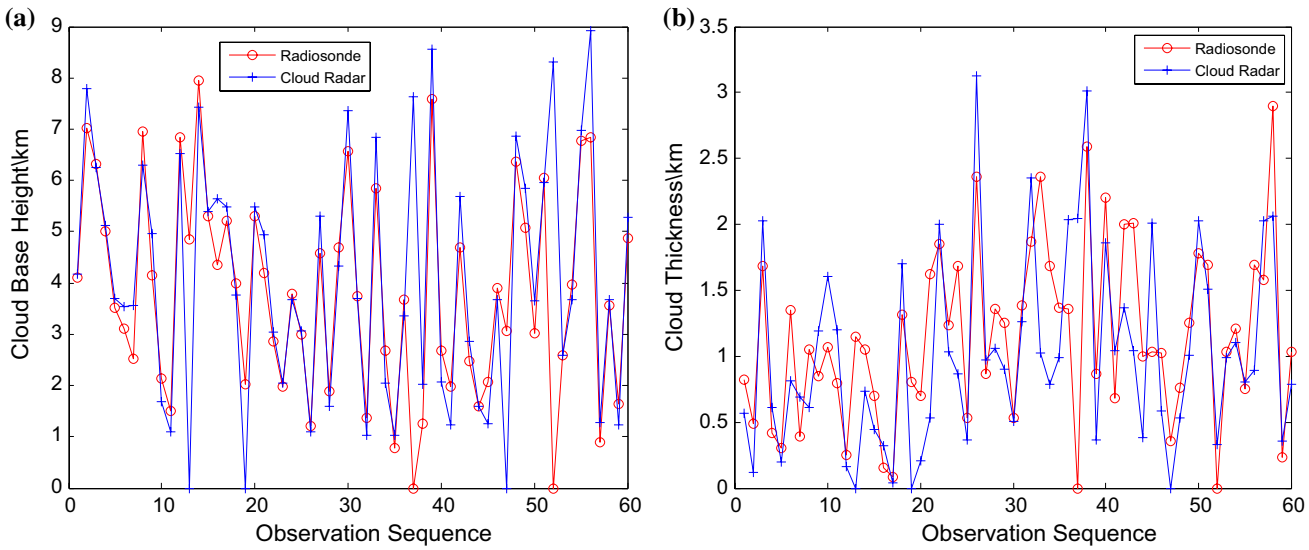

Fig. 1 Comparison of cloud information: **a** cloud base height (km), **b** cloud thickness (km)

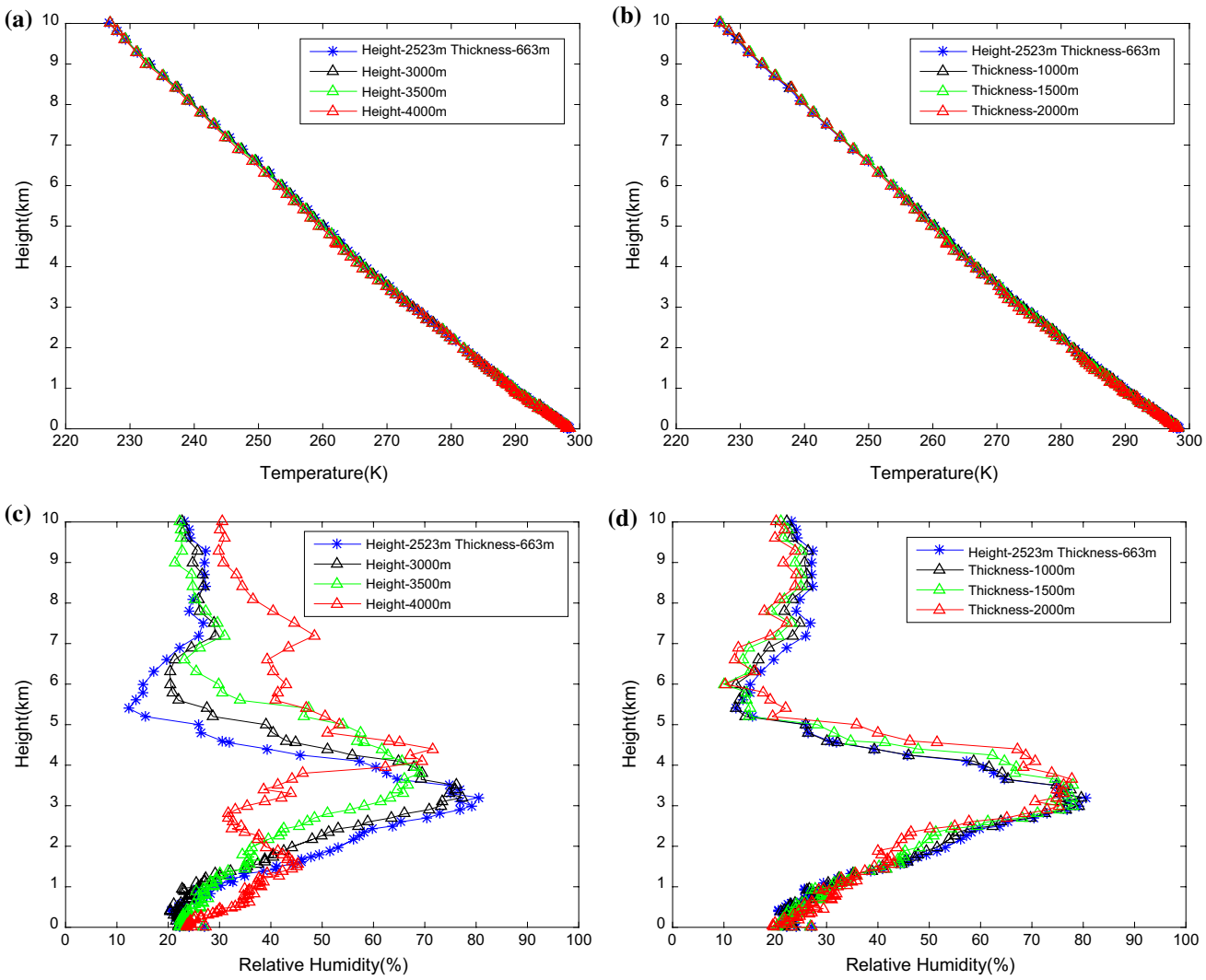

Fig. 2 Case of low-cloud condition

In Fig. 3, the cloud base height is 5027 m and thickness is 915 m in reality. In (a) and (c), we only modify the cloud base height to 4500, 4000, and 3000 m. In (b) and (d), the thickness is modified to 1500, 2000, and 3000 m.

It could be seen that the effects of different cloud height and cloud thickness on temperature profiles are not obvious. However, for relative humidity, the modified cloud height makes a significant change to the relative humidity on the setting cloud height, and the peak of relative humidity has a significant change with the setting cloud height. The modified thickness also makes relative humidity increase significantly on the cloud layers.

According to sample statistics in the paper, the mean error between cloud-based height measured by cloud radar and estimated by radiosonde data is 0.476 km, and for the cloud thickness, it is 0.450 km. As showed in the above two cases, the blue line is atmospheric profile retrieval by the real cloud condition, and the black line is the retrieval when estimating cloud height or thickness exist about 500 m error. For temperature profiles, it could be seen that the blue lines and black lines are very close, and it has little effect on the temperature profile. In addition, for humidity profiles, the error of input cloud mainly affects relative humidity at the cloud layer, while the other heights are much less affected. Different cases may have different deviations, but the maximum error is within 10%.

2.4 Simulating BT measurements based on MonoRTM

Because of the limitations on the number of BT measurements obtainable using the MWR and the necessary inclusion of substantial quantities of BT data during the retrieval process, we simulated BT data based on the monochromatic

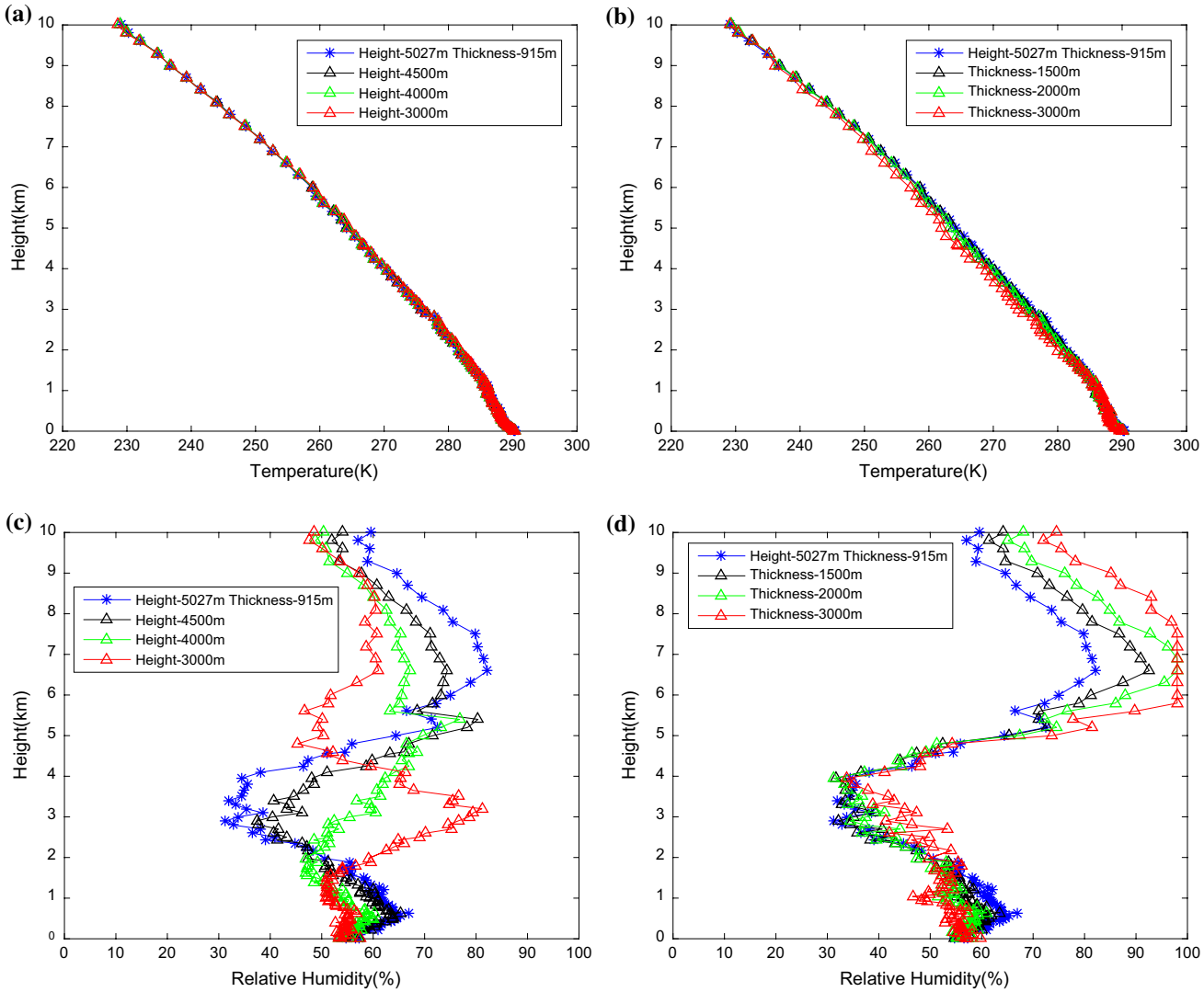

Fig. 3 Case of high-cloud condition

radiative transfer model (MonoRTM) (Clough et al. 2005). The model was provided by Atmospheric and Environmental Research, Inc., and it uses the same physics and continuum model as the line-by-line radiative transfer model (Clough et al. 1992). MonoRTM is suitable for the calculation of radiances associated with atmospheric absorption by molecules in all spectral regions and of the cloud liquid water content in the microwave region. The model uses the Humlicek Voigt line shape and the MT-CKD continuum (Mlawer et al. 2012) to handle molecular absorption that is not included in the "line center" of each spectral line.

The BT calculations for the same channels in the ground-based MWR were obtained by applying MonoRTM to the radiosonde data for Beijing during the period 2006–2013. The sounding data were pre-processed according to the input requirements of MonoRTM. The data were divided into two weather conditions: clear-sky and cloudy. For clear-sky conditions, the simulated BT data could be obtained after the input of the pre-treated sounding profile into MonoRTM. For cloudy conditions, the model required the cloud liquid water content at the height of the cloud layer prior to calculating the BT. However, the required cloud liquid water profiles were not available from conventional upper-air ascent data. Therefore, they were assumed to take the form as noted in Poore et al. (1995) and Tan et al. (2011).

To verify the accuracy of MonoRTM, the BT results were compared with the observations from the MWR. The BT estimates in the 22.24 and 58 GHz channels were consistent with the observations, as shown in Fig. 4.

The BT was simulated using 60 statistical groups in comparison with the measurements acquired by the MWR. Among the 60 samples, 18 samples were acquired during clear-sky conditions and 42 samples were collected under cloudy conditions. It should be noted that precipitation

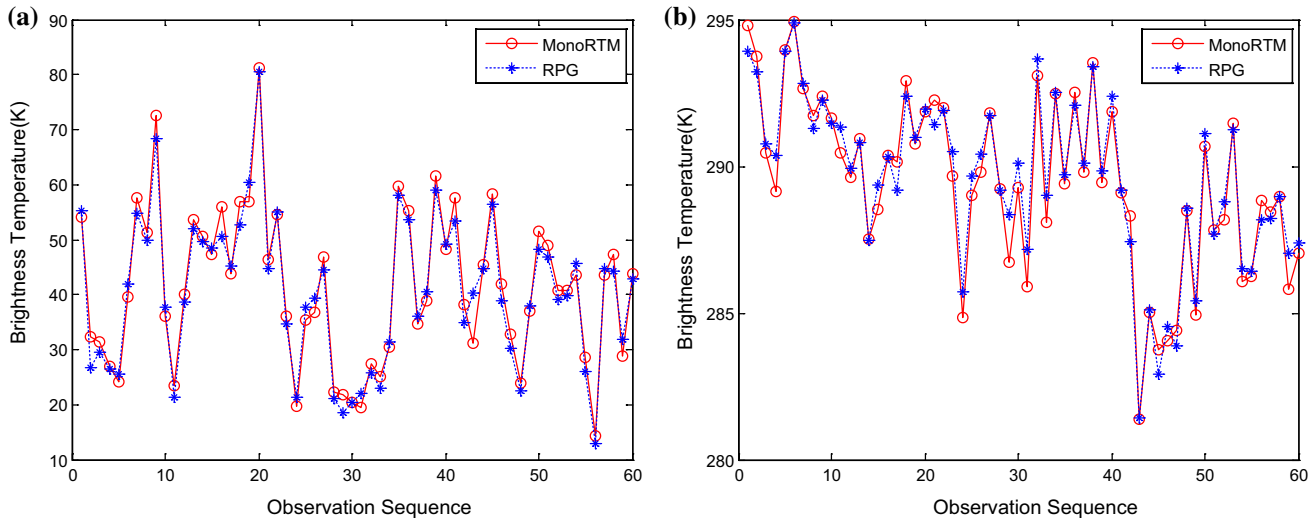

Fig. 4 Comparison of MonoRTM-derived BT estimates and BT observations using the MWR in the **a** 22.24 GHz channel; and **b** 58 GHz channel

Table 1 Statistical comparison between the simulated BT estimates and MWR BT measurements

Frequency (GHz)	Mean deviation (K)	Standard deviation (K)	Correlation coefficient
22.24	2.145	2.508	0.984
23.04	1.988	2.338	0.984
23.84	1.628	2.003	0.983
25.44	1.213	1.662	0.976
26.24	1.065	1.498	0.974
27.84	0.991	1.477	0.963
31.40	1.084	1.672	0.937
51.26	1.590	2.403	0.900
52.28	1.298	1.913	0.909
53.86	0.495	0.680	0.967
54.94	0.350	0.397	0.988
56.66	0.360	0.463	0.987
57.30	0.396	0.513	0.985
58.00	0.455	0.574	0.981

clouds and clouds with very rich liquid water contents were not considered. The accuracy was quantified via the mean deviation (MD), standard deviation (SD), and correlation coefficient (ρ). The statistical results are shown in Table 1.

The maximum MD value between the simulated BT estimates and MWR BT measurements was 2.145 K, and the SD of the MD was 2.508 K. The correlation coefficient was greater than 0.9 for all channels. It is important to note that the radiosonde and MWR were not positioned in the same place, and the sounding balloon may have drifted farther with increasing altitude. Nonetheless, despite the existence of these individual errors, the deviation in the statistical data was acceptable.

3 Retrieval methodology

3.1 BPNN

3.1.1 Principle

There is no need to create a new and complicated algorithm, because the BPNN can theoretically approximate any complex nonlinear relationship. Neural networks have been widely applied to generate atmospheric parameters of inversion profiles. The algorithm uses a standard feed forward network with input, hidden, and output layers that are fully connected between adjacent layers. A standard back-propagation algorithm is used for training, and the standard feed forward network is used for the profile determination (Cimini et al. 2006). As shown in Churnside et al. (1994), we used a three-layer BPNN, which can obtain any precision of a continuous function. A diagram of the BPNN is shown in Fig. 5.

In Fig. 5, L denotes the number of elements in the input layer, M is the number of elements in the hidden layer, and N is the number of elements in the output layer.

The expression of the tansig transfer function, which is used from the input layer to the hidden layer, is

$$\text{tansig}(n) = \frac{2}{1 + \exp(-2 * n)} - 1. \tag{1}$$

Therefore, the relationship between the hidden layer and the input layer can be expressed as

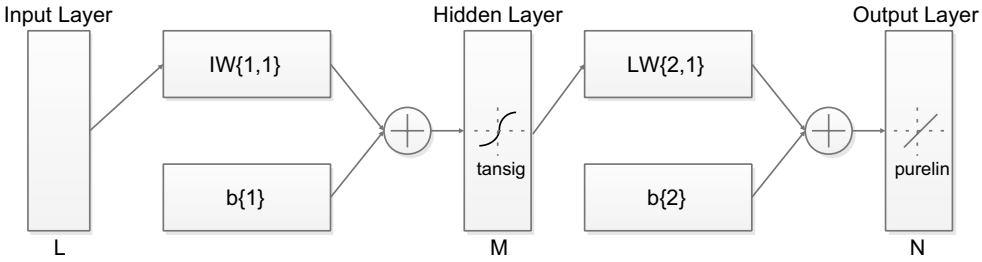

Fig. 5 Schematic diagram of the BPNN

$$Y_j = \text{tansig}\left(\sum_{i=1}^{L} w_{ij}X_i + b_j\right), \tag{2}$$

where Y_j is the jth element of the hidden layer, X_i is the jth element of the input layer, w_{ij} is the weight of X_i to Y_j, and the bias value is represented by b_j.

The linear transfer function purelin is used from the hidden layer to the output layer, and the relationship is written as

$$Z_k = \sum_{j=1}^{M} w_{jk}Y_j + b_k. \tag{3}$$

The weights and biases are determined during the training process. The algorithm adjusts the weights and biases iteratively to reduce the differences between the output vectors of the actual training set and the estimated output vectors calculated by the network using the input vectors of the training set.

3.1.2 Methodology for a comparison with the addition of cloud

To better analyze the impacts of cloud parameters on the retrieval of atmospheric profiles, we fixed the other input parameters and used the cloud base height and cloud thickness as independent channels to input into the BPNN. The information was added to train the network and to build a new neural network model. The results of this new model were then compared with the retrievals without cloud information.

In the inversion model without cloud information [BPNN(No-cloud)], the input vector comprised 17 elements. The first 14 elements were the BT data in 14 radiometer channels. The 15th, 16th, and 17th elements were the surface temperature, relative humidity, and pressure, respectively. The output vectors were 47-element vertical profiles of either the temperature or the relative humidity. The vertical resolution was 100 m between the heights of 0 and 1 km and 125 m between the heights of 1 and 10 km.

In the inversion model with cloud information [BPNN(Cloud)], the output vectors were the same as those in the model without cloud information. However, the input vector included two more elements than the model without cloud information. The first 17 elements were the same as those in the model without cloud information, and the final elements were the cloud base height and cloud thickness.

Using the two abovementioned models, all of the samples were trained using different methods to obtain two different parameters of the neural network possessing different input elements and identical output elements. The test sample should be input using the requirements of the input layer for the different models.

3.2 RPG-HATPRO retrieval method

To estimate the atmospheric profiles from the radiometer data, the RPG-HATPRO radiometer has its own retrieval algorithm. The manufacturer's software provides three selectable retrieval types: linear regression, quadratic regression and neural network. The retrieval type utilized in this experiment was quadratic regression.

The quadratic regression retrieval calculation has the following structure:

$$\begin{aligned}\text{Out}_i = &\text{OS}_i + \sum_{\text{sensors}} \text{SL}_{ij} * \text{Sr}_j + \sum_{\text{freq}} \text{TL}_{ij} * \text{Tb}_j \\ &+ \sum_{\text{sensors}} \text{SQ}_{ij} * \text{Sr}_j^2 + \sum_{\text{freq}} \text{TQ}_{ij} * \text{Tb}_j^2,\end{aligned} \tag{4}$$

where Out_i is the ith retreival output parameter, OS_i is the retrieval offset parameter for Out_i, Sr_j is the surface sensor reading of the jth checked sensor (the sequence for which is as follows: temperature sensor, humidity sensor, pressure sensor, and infrared radiometer), SL_{ij} is the corresponding linear coefficient, SQ_{ij} is the corresponding quadratic coefficient, Tb_j is the brightness temperature at the jth frequency, TL_{ij} is the corresponding linear coefficient, and TQ_{ij} is the corresponding quadratic coefficient.

The quadratic regression retrieval process also used nearly 10 years of sounding data as the database, but the sounding data used for the RPG retrieval were provided by the University of Wyoming (online at http://weather.uwyo.edu/upperair/sounding.html). The corresponding simulated radiometer BT data were also calculated using MonoRTM.

Through the relationship correlating the calculated BT, sensor, and sounding data, the coefficients of the quadratic regression were obtained. In addition, the coefficients were applied to the radiometer measurements to retrieve the actual atmospheric variables.

4 Influence of cloud information on the retrieval

4.1 Theory

When considering a plane-parallel atmosphere, scattering can be ignored and the zenith angle in the direction of radiative transfer is given as θ. For ground-based remote sensing, the atmospheric downward radiance that is received can be expressed as in Tan et al. (2011):

$$T_{B\beta}^{\downarrow}(\theta,0) = T_{B\beta}(\infty)\tau(0,\infty) + \int_0^{\infty} k_{\alpha}(z)T(z)\tau(0,z)\sec\theta \mathrm{d}z. \tag{5}$$

In the above equation, $T_{B\beta}(\infty)\tau(0,\infty)$ refers to the cosmic radiation in the background after experiencing attenuation in the atmosphere, where the quantity $T_{B\beta}(\infty)$ is the cosmic background temperature, usually taken to be 2.75 K, $\tau(0,z)$ is the transmittance from the height z to the ground; $T(z)$ is the atmospheric temperature at the height z, and k_{α} is the atmospheric absorption coefficient. Under clear-sky conditions, the absorption coefficient mainly results from absorption by oxygen molecules and water vapor, and it can be expressed by $k_{\alpha} = k_{\mathrm{O_2}} + k_{\mathrm{H_2O}}$. However, under cloudy conditions, the calculation of the atmospheric absorption coefficient is different. The cloud layers, including cloud liquid water, impact the absorption coefficient substantially. Under cloudy conditions, the absorption coefficient can be expressed as: $k_{\alpha} = k_{\mathrm{O_2}} + k_{\mathrm{H_2O}} + k_{\mathrm{cloud}}$.

The existence of cloud layers can change the BT measured by the MWR. Research has shown that differences in the cloud height, cloud thickness, and density of cloud liquid water have different effects on BT measurements. However, the provision of cloud physical parameters by the MWR is poor during the retrieval of atmospheric profiles. To obtain cloud information, the MWR itself is configured with far-infrared radiometer components that can measure the infrared radiation brightness temperature of the sky to judge the existence of clouds and estimate the cloud base height. However, because of the impacts of numerous factors, such as the atmosphere, aerosols, and cloud structure, the cloud base height measured using an infrared sensor requires error testing, and it is difficult to obtain accurate data in the long term. Moreover, the cloud base height, the cloud thickness, the distribution of cloud liquid water, and even the particles within clouds may all have considerable impacts on the retrieval. Because the cloud information that the retrieval process requires is lacking, the inversion of temperature and humidity profiles could produce large errors in the cloud estimations.

Therefore, we combined active and passive remote sensing techniques and built a joint observation system that includes both the MWCR and the MWR. In addition, additional high-accuracy cloud information from the cloud radar was added into the process of retrieving the atmospheric profiles using the BPNN as the key tool. The accuracy of the retrieval results was analyzed through a comparison with L-band sounding radar data. Based on the above approach, the impact of the inclusion of cloud information on the retrieval of atmospheric profiles was assessed.

4.2 Typical cases

In this section, radiosonde data are used as a standard and compared with both the BPNN retrieval profiles (both with and without cloud information) and the RPG retrieval results. To compare the results from the three retrieval methods with the radiosonde measurements more intuitively, we present four typical cases of temperature (Fig. 6) and relative humidity (Fig. 7) profiles at different times under cloudy conditions. It is mainly considered to include a variety of cloud categories when selecting the display cases, so the following four typical cases include low, medium, and high cloud conditions.

As seen from the four typical cases, the three retrieved temperature profiles (Fig. 6) are relatively similar to the sounding data from the ground to a height of 5 km. However, the deviation in the RPG product increases considerably at heights above 5 km, and the differences between the temperatures from the BPNN(No-cloud) model and those from the radiosonde increase above 8 km. Although the BPNN(Cloud) model also shows a deviation from the radiosonde data above 9 km, the deviation is clearly lower than those for the other two methods.

The retrievals using the different methods are far more variable for the relative humidity (Fig. 7) than those for the temperature. The RPG product can approximately follow the patterns of the radiosonde data with changes in the height, but the deviation clearly increases with the inclusion of cloud information, and the trend with increasing height is not the same as that in the sounding data. In addition, the bias in the BPNN(No-cloud) model is large above the cloud height, but this issue is substantially improved after adding cloud information.

4.3 Statistical analysis

The accuracies of the retrieved atmospheric profiles were quantified statistically through a comparison with the actual

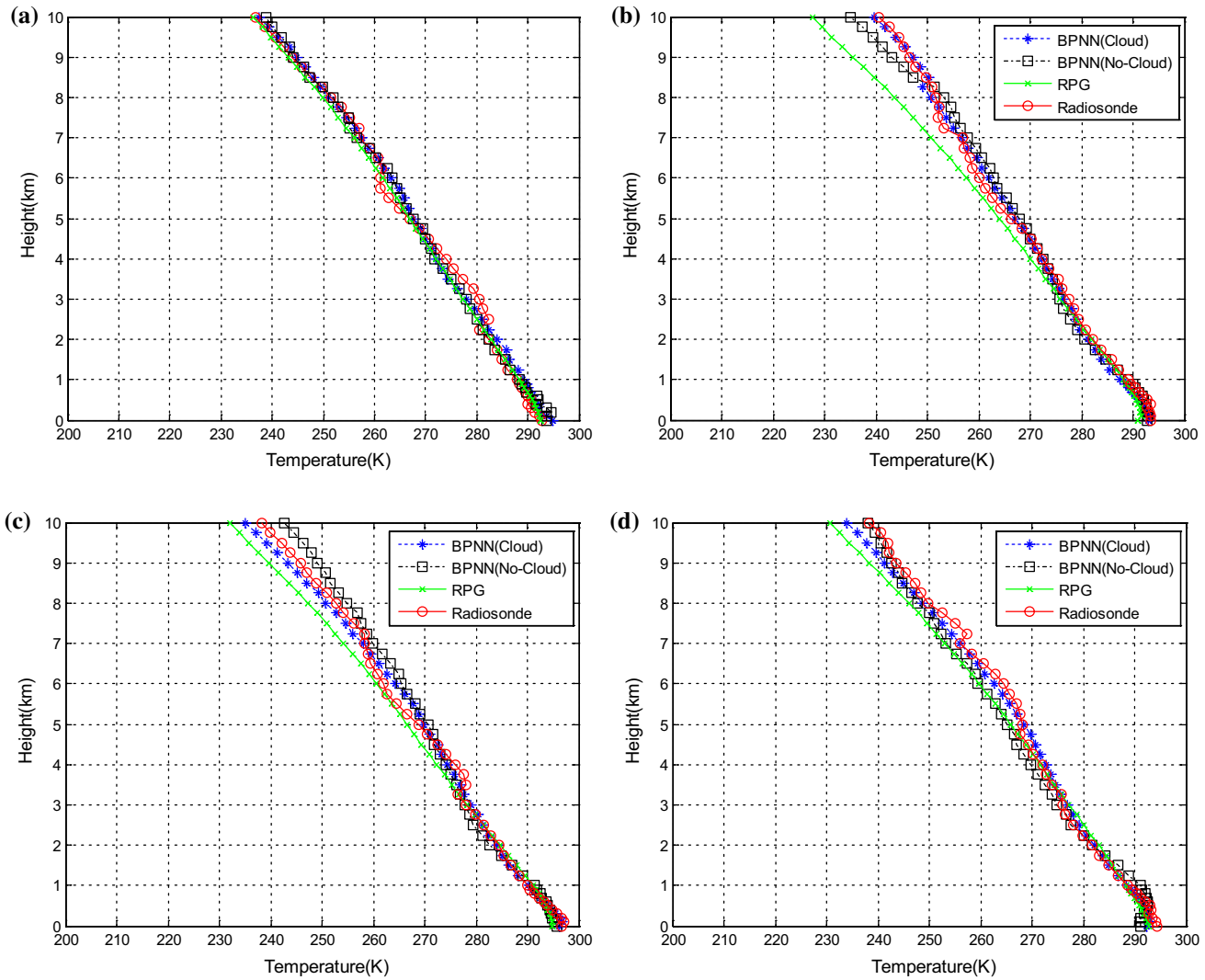

Fig. 6 Comparison between the temperature profiles generated using the BPNN(Cloud) and BPNN(No-cloud) inversion models, the PRG product and the radiosonde at **a** 23:15 UTC on 06 November 2014, **b** 23:15 UTC on 03 October 2014, **c** 23:15 UTC on 02 November 2014, and **d** 11:15 UTC on 08 October 2014

radiosonde measurements in terms of the mean bias (MB), root-mean-square error (RMSE), and correlation coefficient (ρ). The MB and RMSE were used to evaluate the deviations between the retrieved parameters and the sounding data for each height layer. The value of the correlation coefficient indicates the difference between each retrieval profile, which are organized according to the 47 height layers, and the corresponding sounding data.

The 382 groups of sounding data from 2014 to January 2015, excluding rainy conditions, were used as independent data sets in the analysis of the accuracy of the retrieval profiles using the three methods. The results are shown in Fig. 8.

Figure 8 shows that, during the temperature retrieval, the MB in BPNN(Cloud) fluctuated between − 0.9 and 0.6 K, while the RMSE varied between 0.2 and 3.2 K. Meanwhile, the MB in BPNN(No-cloud) fluctuated between − 1 and 1.1 K, and the RMSE increased from 0.5 to 3.6 K over the height range of 0–10 km. The MB in the MWR data varied substantially between − 1 and − 6 K, while the RMSE increased from 0.3 to 6.5 K with a more rapid increase above 7 km.

In the retrieved humidity profiles, the MB in BPNN(Cloud) fluctuated between − 6 and 7%; the RMSE increased rapidly from 2.5 to 24% from the ground to 6 km, and the RMSE was 6–22% above 6 km. The MB in BPNN(No-cloud) fluctuated between − 9 and 7%, while the RMSE had already increased to 27% at 3.5 km and then oscillated between 15 and 27% from 2.5 to 10 km. The MB in the RPG product results was 1–15%, while the RMSE increased to 31% from 0 to 3.5 km and then fluctuated in oscillations down to 22.5% at 10 km.

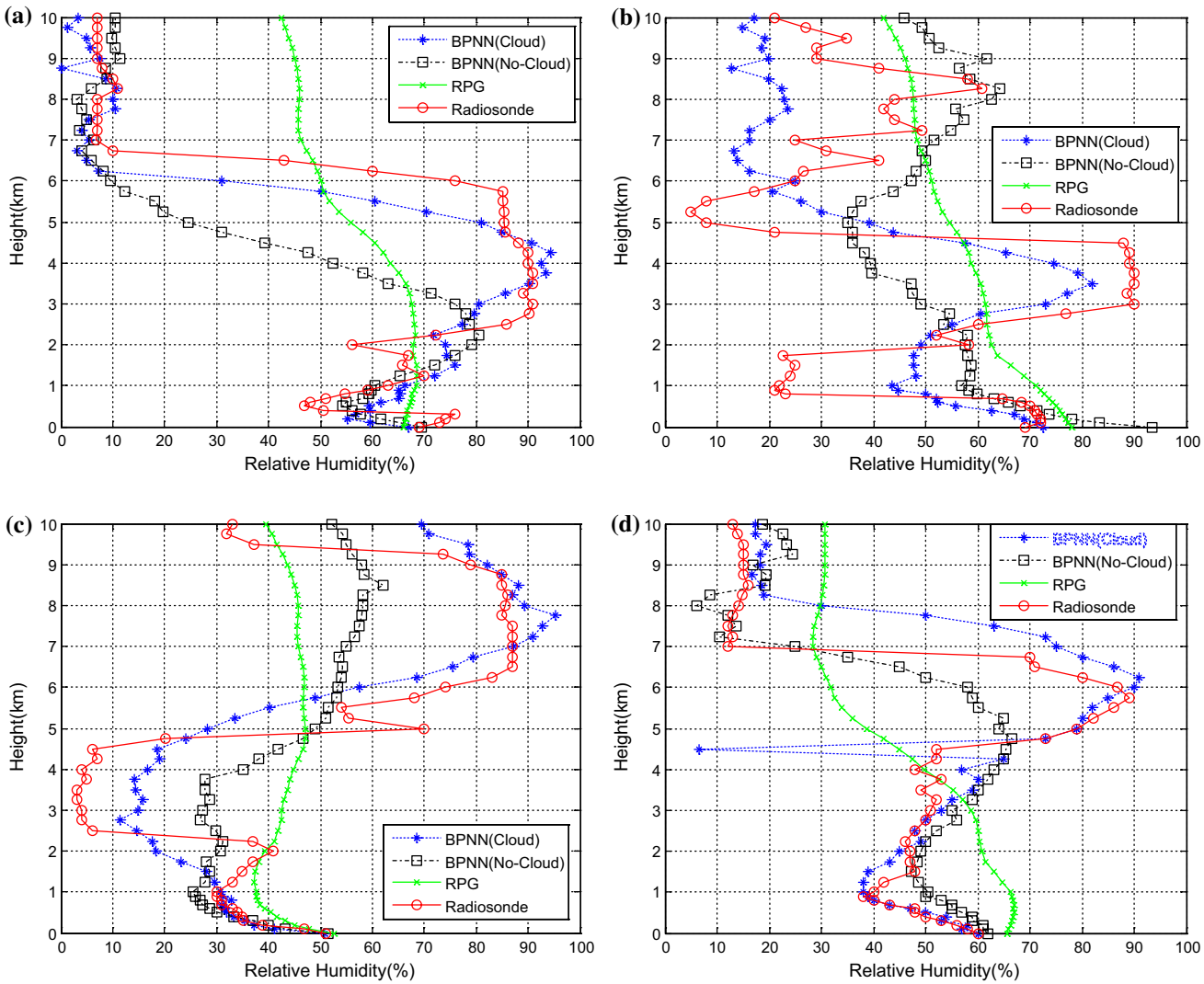

Fig. 7 Comparison between the relative humidity profiles generated using the BPNN(Cloud) and BPNN(No-cloud) inversion models, the RPG product and the radiosonde at **a** 23:15 UTC on 06 November 2014, **b** 23:15 UTC on 03 October 2014, **c** 23:15 UTC on 02 November 2014, and **d** 11:15 UTC on 08 October 2014

The RMSE statistics showed that the temperature profiles roughly conform to the characteristics of the ground-based remote sensing data. The retrieval accuracy gradually reduced from the ground to 10 km. However, the humidity profiles showed large differences with an increase in the height. To analyze the impacts of cloud information more clearly, we considered the RMSEs between BPNN(Cloud) and BPNN(No-cloud) separately according to differences in the cloud base height. The cloud samples were divided into three categories following the work of China Meteorological Administration (2007): low-cloud, mid-cloud, and high-cloud heights. A low-cloud height is defined when the cloud base height is under 2.5 km, a mid-cloud height is within 2.5–4.5 km, and a high-cloud height is above 4.5 km. The number of low-cloud samples was 70, that of mid-cloud samples was 63, and that of high-cloud samples was 62. The results are shown in Fig. 9.

As the comparison of the humidity profiles under different cloudy conditions shown in Fig. 9, the RMSE increased obviously at heights between 1.5 and 5 km at low-cloud

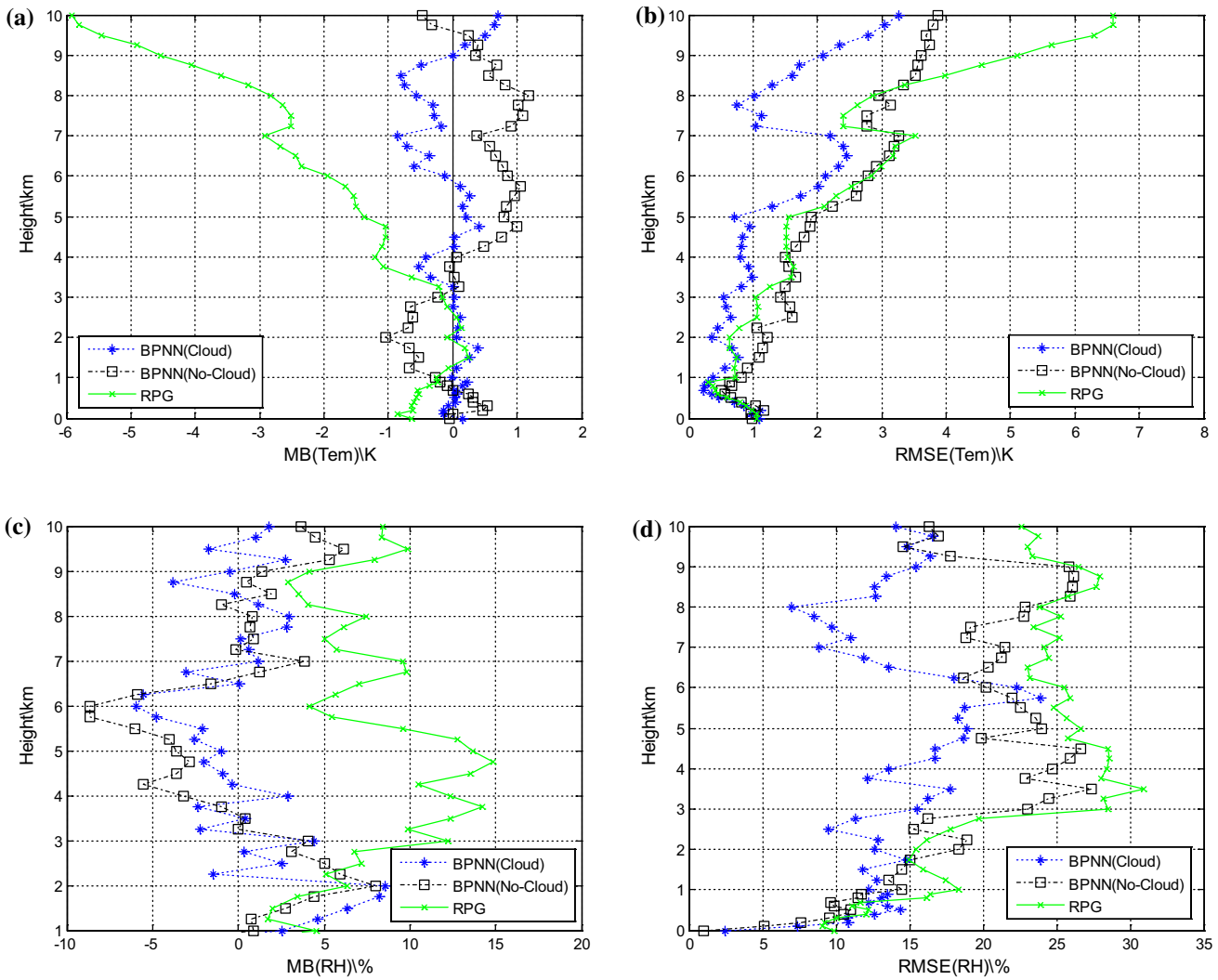

Fig. 8 Using radiosonde data as a standard, comparison of the BPNN(Cloud) and BPNN(No-cloud) inversion models, the RPG product for the **a** MB of the temperature profiles, **b** RMSE of the temperature profiles, **c** MB of the humidity profiles, and **d** RMSE of the humidity profiles

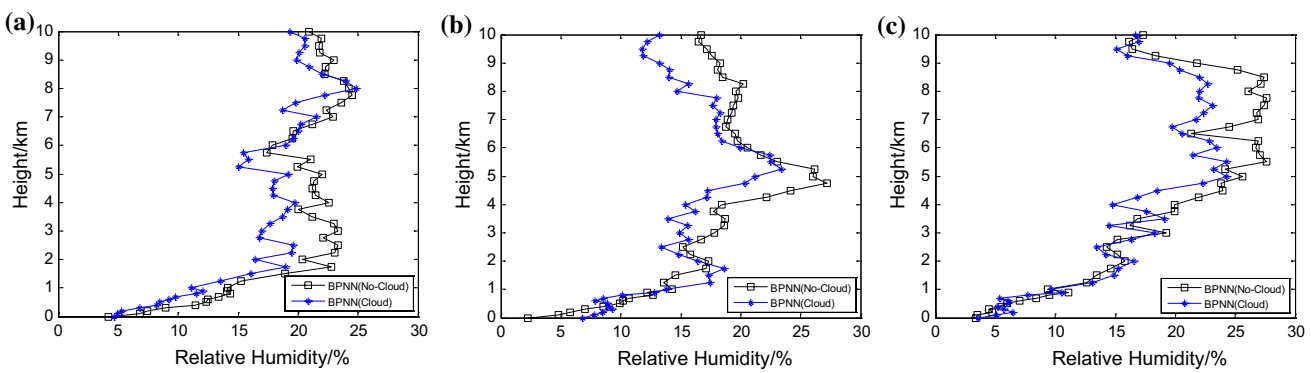

Fig. 9 Using radiosonde data as a standard, comparison of RMSEs among the humidity profiles from the BPNN(Cloud) and BPNN(No-cloud) models under different cloudy conditions: **a** low-cloud; **b** mid-cloud; and **c** high-cloud heights

heights, but at mid-cloud heights, the maximum RMSE values appeared at approximately 5 km. Meanwhile, the RMSEs above 5 km at high-cloud heights were obviously larger than those in the other two categories. After the addition of cloud information, BPNN(Cloud) showed a clear improvement above the cloud layers, but it could not change the RMSE trend with an increase in the height. Therefore, the results indicate that the presence of clouds could cause obvious errors at and above the cloud height; moreover, the addition of cloud information can amend these errors but cannot eliminate them.

To quantify the three retrieved profiles, we also randomly selected 75 samples from cloudy conditions to facilitate a comparison of the correlation coefficients with the corresponding sounding data. The results are shown in Fig. 10.

For the retrieved temperature profiles, the average correlation coefficient between BPNN(No-cloud) and the radiosonde data was 0.990, while that between BPNN(Cloud) and the radiosonde data was 0.994. The average correlation coefficient between the RPG product and radiosonde profiles was 0.992.

For the relative humidity profiles, the average correlation coefficient between BPNN(No-cloud) and the radiosonde data was 0.685, while that between BPNN(Cloud) and the radiosonde data was 0.805. After the addition of cloud information, 49 out of the 75 samples showed an improved correlation. The maximum increase in the correlation coefficient was 0.330, and the average correlation coefficient between the RPG product and radiosonde profiles was 0.657.

5 Advantage of the MWCR

The results from the four typical cases demonstrate that the temperature and humidity profiles retrieved using the MWR show almost identical trends to the radiosonde data but do not show a good response in layers with clouds. Furthermore, the MB and RMSE statistics indicate that the deviation increases significantly above 3 km. However, the retrievals using the BPNN with the addition of cloud parameters were much better, especially as the BPNN is able to reflect the significant increase in the relative humidity in cloudy layers.

To analyze the reasons for these results, we next compared data from the MWCR with the cloud base heights observed using the far-infrared radiometer components from the MWR self. The time chosen by cases is the entire cloud process from generation to extinction corresponding to the cases in Sect. 4.2. It should be noted that the cloud base height of the far-infrared component is set to 10 km when it does not detect clouds.

Figure 11 shows that the cloud base height in case b obtained via far-infrared remote sensing is similar to that

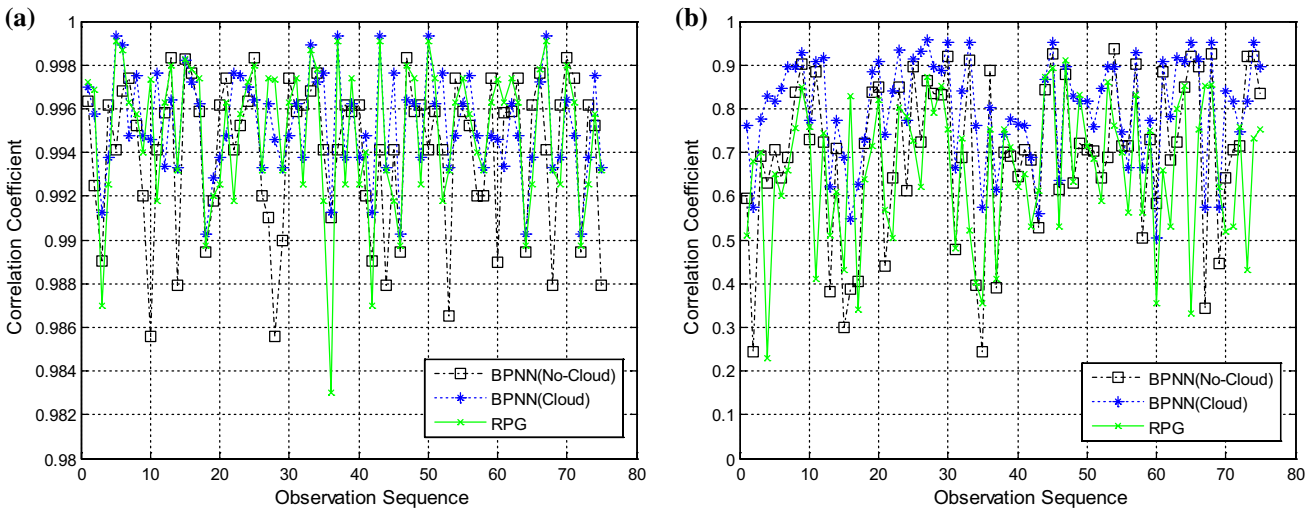

Fig. 10 Using radiosonde data as a standard, comparison of the correlation coefficient among BPNN(Cloud) and BPNN(No-cloud) inversion models, the RPG product for **a** temperature profiles; and **b** relative humidity profiles

acquired using the cloud radar. However, in cases a, c, and d, there is a considerable difference between the cloud parameters measured by the two instruments. Slight fog or haze was observed during the sounding times of cases a and c, and the cloud base height obtained using the far-infrared radiometer was measured at a height of 1 km or less at the time. Meanwhile, thin cloud conditions were observed at the sounding time of case d, but the far-infrared radiometer did not detect the existence of clouds.

When there were high levels of fog, haze, or relative humidity at the surface, the MWR could not detect the existence of high-altitude clouds because of the weather, and the obtained cloud base height may show large deviations or considerable errors. For thin clouds, there may also be missing data in the MWR data set. However, according to Sect. 4.1, the existence of cloud layers could change the BT measured using the MWR, and thus, cloud base height determinations are insufficient for the retrieval of atmospheric profiles. Moreover, measurements of the cloud base height sometimes show large deviations, indicating that large errors exist in the retrievals of profiles under cloudy conditions.

In contrast, when using a combination of MWR and cloud radar observations, the MWCR uses cloud particle scattering properties of electromagnetic waves. We could, therefore, analyze radar echoes to obtain the various features of clouds, which can then reflect their macroscopic and microscopic structures. From this, we could obtain the cloud base height more accurately. Cloud radar can also be used to obtain the cloud thickness, cloud cover and even microphysical parameters of clouds, thereby providing a more complete set of cloud parameter information for the retrieval process. However, because of the short time period of combined observations, the quantity of cloud radar data is limited, and thus, the cloud base height and cloud thickness estimates in a part of the training sample need to be estimated via sounding data. Unfortunately, in this study, the radiosonde was unable to provide accurate cloud information, with the exception of cloud base height and cloud thickness measurements; therefore, we were able to add only two channels (i.e., the cloud height and thickness) in the final retrieval. We aim to solve this problem in future research.

6 Conclusions

This study used a combination of active and passive remote sensing techniques to tackle the increased bias in MWR retrievals during cloudy conditions. Cloud base height and cloud thickness measurements obtained using the MWCR were applied to the retrieval of atmospheric profiles. We compared the retrieved profiles (both with and without cloud information) and the product of a radiometer with sounding data. To analyze the resulting biases, we compared the cloud radar data with the cloud base heights using the far-infrared radiometer of the MWR at the same time. The key conclusions can be summarized as follows.

It should be noted that the network training by radiosonde data and cloud radar could only be used in Beijing or surrounding area, because nearly 10 years Beijing radiosonde data using in the algorithm can only reflect the Beijing climate change. The re-training for the local radiosonde data is needed if we want to use the new algorithm to improve the retrieval of other sites. However, the method of retrieval could be in common use.

1. The three retrieval methods essentially exhibited consistent results in terms of their error trends for the temperature and relative humidity profiles with varying height. The accuracies of the retrievals were high near the ground, and they decreased with height. This confirms the detection performance of the ground-based MWR.
2. A comparison between the MWCR and the far-infrared radiometer components configured using the MWR showed that the latter was able to obtain the cloud base height but struggled to measure this parameter steadily in the long term, because the data quality was negatively affected by the weather conditions.
3. The precisions of the retrieval without clouds and the MWR product were significantly reduced in cloudy layers, but their precisions significantly improved after the addition of accurate information from the cloud radar. Compared with the retrieval without cloud information, the retrieved temperature and humidity profiles were more similar to the radiosonde data after cloud information was added for the cloudy layers. This improvement was especially clear in the upper layers.

This study analyzed the causes of increased deviations detected using the MWR during periods of cloudy conditions and then integrated MWCR measurements to improve the data. The results verify that the use of accurate cloud information to improve the retrieval accuracy is a feasible approach. In future experiments, we will combine long-term cloud radar and MWR observations and employ more abundant cloud distribution information to

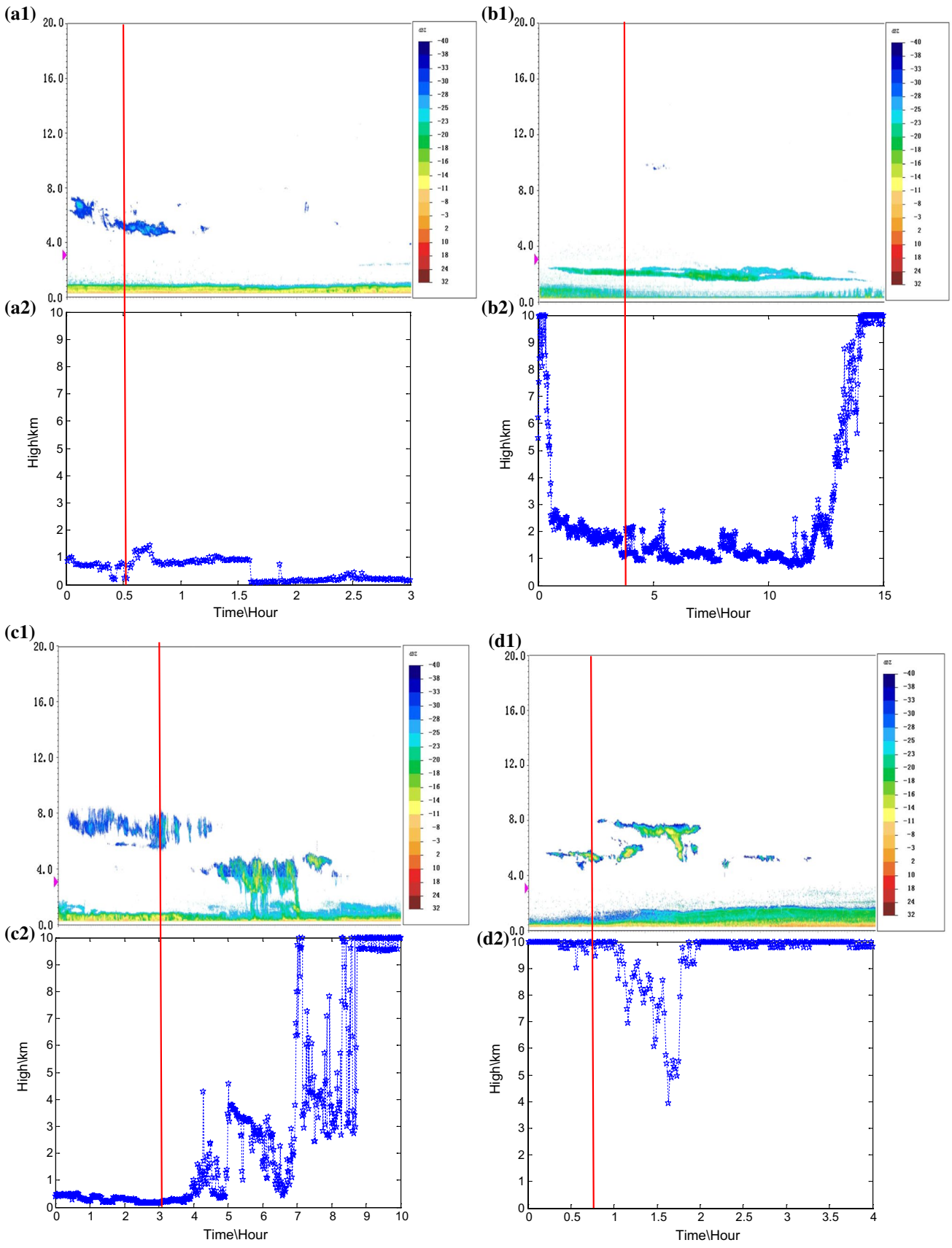
(a1)
(b1)
(a2)
(b2)
(c1)
(d1)
(c2)
(d2)
High\km
Time\Hour
dBZ

◂**Fig. 11** Comparison of reflectivity of cloud radar (**a1**–**d1**) and the cloud base heights observed using far-infrared radiometer components from MWR self (**a2**–**d2**) on **a** 06 November 2014, **b** 03 October 2014, **c** 02 November 2014, and **d** 03 October 2014. The red line is the time of the radiosonde data

improve the BT retrieval algorithm using the MWR and obtain a more complete vertical profile.

Acknowledgements This research received funding from the Key Program (2015Z001) of the CAMS. The authors would like to acknowledge and thank Li Liang, Xiaohu Pu, and Fa Tao for their work in improving the manuscript.

References

Bian J, Chen H, Vmel H (2011) Intercomparison of humidity and temperature sensors: GTS1, Vaisala RS80, CFH. Adv Atmos Sci 28(1):139–146

Bianco L, Cimini D, Marzano F, Ware R (2005) Combining microwave radiometer and wind profiler radar measurements for high-resolution atmospheric humidity profiling. J Atmos Ocean Technol 22:949–965

Brandau C, Russchenberg H, Knap W (2010) Evaluation of ground-based remotely sensed liquid water cloud properties using shortwave radiation measurements. Atmos Res 96:366–377

Candlish L, Raddatz R, Asplin M et al (2012) Atmospheric temperature and absolute humidity profiles over the beaufort sea and amundsen gulf from a microwave radiometer. J Atmos Ocean Technol 29:1182–1201

Chan P (2009) Performance and application of a multi-wavelength, ground-based microwave radiometer in intense convective weather. Meteorol Z 18:253–265

China Meteorological Administration (2007) Specifications for surface meteorological observation (QX/T 48-2007). China Meteorological Press, Beijing, pp 11–16

Churnside J, Stermitz T, Schroeder J et al (1994) Temperature profiling with neural network inversion of microwave radiometer data. J Atmos Ocean Technol 11(1):105–109

Cimini D, Hewison T, Martin L et al (2006) Temperature and humidity profile retrievals from ground-based microwave radiometers during TUC. Meteorol Z 15:45–56

Clough S, Iacono M, Moncet J et al (1992) Line-by-line calculation of atmospheric fluxes and cooling rates: application to water vapor. J Geophys Res 97:15761–15785

Clough S, Shephard M, Mlawer EJ et al (2005) Atmospheric radiative transfer modeling: a summary of the AER codes. J Quant Spectrosc Radiat Transf 91:233–244

Frate F, Schiavon G (1998) A combined natural orthogonal function/neural network technique for the radiometric estimation of atmospheric profiles. Radio Sci 33(2):405–410

Frisch A, Fairall C, Snider J et al (1995) Measurement of stratus cloud and drizzle parameters in ASTEX with Ka-band Doppler radar and microwave radiometer. J Atmos Sci 52:2788–2799

Han Y, Westwater E (1995) Remote sensing of tropospheric water vapor and cloud liquid water by integrated ground-based sensors. J Atmos Ocean Technol 12:1050–1059

Klaus V, Bianco L, Gaffard C et al (2006) Combining UHF radar wind profiler and microwave radiometer for the estimation of atmospheric humidity profiles. Meteorol Z 15:87–97

Lijegren J, Clothiaux E (2001) A new retrieval for cloud liquid water path using a ground-based microwave radiometer and measurements of cloud temperature. J Geophys Res D13:14485–14500

Lohnert U, Crewell S, Simmer C et al (2001) Profiling cloud liquid water by combining active and passive microwave measurements with cloud model statistics. J Atmos Ocean Technol 18:1354–1366

Mlawer E, Payne V, Moncet J et al (2012) Development and recent evaluation of the MT-CKD model of continuum absorption. Philos Trans R Soc 370:1–37

Poore K, Wang J, Rossow W (1995) Cloud layer thicknesses from a combination of surface and upper-air observations. J. Clim 8:550–568

Sanchez J, Posada R, Garcia-Ortega E et al (2013) A method to improve the accuracy of continuous measuring of vertical profiles of temperature and water vapor density by means of a ground-based microwave radiometer. Atmos Res 122:43–54

Solheim F, Godwin J, Westwater E et al (1998) Radiometric profiling of temperature, water vapor and cloud liquid water using various inversion methods. Radio Sci 33:393–404

Stankov B (1996) Ground- and space-based temperature and humidity retrievals: statistical evaluation. J Appl Meteorol 35:444–463

Tan H, Mao J, Chen H et al (2011) A study of a retrieval method for temperature and humidity profiles from microwave radiometer observations based on principal component analysis and stepwise regression. J Atmos Ocean Technol 28:378–389

Wang J, Rossow WB (1995) Determination of cloud vertical structure from upper-air observations. J Appl Meteorol 34:2243–2258

Wang Z, Xu P, Deng J et al (1995) Simulation of atmospheric vapor, liquid water content, and excess propagation path length based on a 3-channel microwave radiometer sensings (in Chinese). J Nanjing Inst Meteorol 18:396–403

Ware R, Solheim F, Carpenter R et al (2003) A multi-channel radiometric profiler of temperature, humidity and cloud liquid. Radio Sci 38:8079

Ware R, Cimini D, Campos E, Giuliani G (2013) Thermodynamic and liquid profiling during the 2010 Winter Olympics. Atmos Res 132–133:278–290